

$\Delta(1232)$ -nucleon interaction in the ${}^2\text{H}(p,n)$ charge-exchange reaction

C. A. Mosbacher and F. Osterfeld

Institut für Kernphysik, Forschungszentrum Jülich GmbH, D-52425 Jülich, Germany

(Received 11 April 1997)

The ${}^2\text{H}(p,n)$ charge exchange reaction at $T_p=790$ MeV is used to study the $\Delta(1232)$ -nucleon (ΔN) interaction in the Δ resonance excitation energy region. For the ΔN potential, a meson exchange model is adopted where π , ρ , ω , and σ meson exchanges are taken into account. The deuteron disintegration below and above pion threshold is calculated using a coupled-channel approach. Various observables, such as the inclusive cross section, the quasifree Δ decay, the coherent pion production, and the two-nucleon breakup, are considered. It is shown that these observables are influenced by the dynamical treatment of the Δ degrees of freedom. Of special interest is the coherent pion decay of the Δ resonance, which is studied by means of the exclusive reaction ${}^2\text{H}(p,n\pi^+){}^2\text{H}$. Both the peak energy and the magnitude of the coherent pion production cross section depend very sensitively on the strength of the ΔN potential. The coherent pions have a peak energy of $\omega=300$ MeV and a strongly forward peaked angular distribution. [S0556-2813(97)00610-9]

PACS number(s): 25.40.Kv, 25.10.+s, 14.20.Gk, 24.10.Eq

I. INTRODUCTION

In recent years, inclusive and exclusive (p,n) and (${}^3\text{He},t$) charge-exchange reactions at intermediate energies have been proven to be excellent probes for investigating the Δ dynamics in nuclei. The most important observation of the inclusive charge exchange reactions is the downward energy shift of the Δ resonance peak position by ≈ 70 MeV in nuclear targets (with mass number $A \geq 10$) as compared to the proton target [1–5]. Microscopic Δ -hole model calculations show that a large part of this shift is caused by the attractive Δ -nucleon (ΔN) interaction in the spin-longitudinal (LO) channel [6–10]. A direct signature of this interaction is provided by the measurement of the coherent pion decay spectrum where the pion of the Δ resonance decay is measured in coincidence with the ejectile while the target nucleus is left in its ground state [11–16]. These coherent pions couple strongly to the LO channel. Due to the attractive ΔN potential in this channel, their energy spectrum is substantially shifted downward relative to the Δ resonance peak position of the inclusive reaction.

In this paper we study the Δ excitation in the deuteron target using the ${}^2\text{H}(p,n)$ charge-exchange reaction at $T_p=790$ MeV. The deuteron has the advantage that its wave function is well known and that the Fermi motion of the ΔN system can be treated properly. Therefore, the effects of the ΔN interaction can be studied in a more direct way than in heavier nuclei. In the past most of the studies on the deuteron have been carried out with electromagnetic and hadronic probes, such as in photon-deuteron (γd) and pion-deuteron (πd) scattering, leading to NN , πd , and πNN final reaction channels. In these reactions the intermediate ΔN interaction plays an important role [17–23]. The photon excites the Δ dominantly with spin-transverse (TR) coupling, i.e., by the transition operator $\vec{S} \times \vec{q} \vec{T}$ (\vec{S} and \vec{T} are the spin and isospin transition operators, respectively), while the pion excites it with spin-longitudinal ($\vec{S} \cdot \vec{q} \vec{T}$) coupling. Both couplings are orthogonal to each other and therefore give different information on the ΔN interaction. In the charge-exchange reac-

tions the target is exposed to the virtual π and ρ meson fields produced by the (p,n) projectile-ejectile system. The pionlike interaction excites the LO response function ($\vec{S} \cdot \vec{q} \vec{T}$ coupling) of the target while the ρ -meson-like interaction excites the TR response function ($\vec{S} \times \vec{q} \vec{T}$ coupling). Due to the kinematics, the virtual meson fields obey the energy-momentum relation $\omega < q$ and thus explore the LO and TR response functions in an (ω, \vec{q}) region that is inaccessible to real pion and real photon scattering.

In the interpretation of the (γd) and (πd) scattering reactions, various theoretical models have been applied to treat the ΔN dynamics. Among these models are the coupled-channel approach [24–29] and the three-body Faddeev treatment of the πNN system [30,31]. In the present paper we make use of a coupled-channel approach to describe the ΔN system in a nonrelativistic framework. We set up a system of coupled equations for the ΔN wave function in configuration space. We then apply the Lanczos method for solving the equations. The ΔN potential is constructed within a meson-exchange model. The exchanged mesons taken into account are the pion (π), the rho (ρ), the omega (ω), and the sigma (σ).

The aim of the present paper is to show that the (p,n) reaction at forward-scattering angles is an interesting tool to study the ΔN interaction in the deuteron. The advantage of the (p,n) reaction over other probes is twofold. First, at forward-scattering angles the quasielastic peak cross section and the Δ resonance peak cross section are energetically well separated. The Δ resonance cross section is very large compared to the quasielastic cross section providing a well-defined Δ resonance peak in the spectrum. Second, the Δ resonance cross section involves both a LO and a TR component (with a ratio of LO/TR=1/2) and thus allows one to examine the complete spin structure of the ΔN interaction. The LO excitation is of special interest for the coherent pion decay of the ΔN system. Due to the LO spin structure in both the excitation and deexcitation process, the cross section for coherent pion production becomes relative large. Because the ΔN interaction is most attractive in the LO chan-

nel, the coherent pion spectrum is expected to exhibit clearly the effects of the ΔN potential. It turns out, indeed, that both the peak energy and the magnitude of the coherent pion production cross section depend quite sensitively on the strength of this potential. Other observables, such as the inclusive cross section, the quasifree Δ decay cross section, and the two-nucleon breakup, are also shown to be influenced by the dynamical treatment of the Δ degrees of freedom.

The organization of the present paper is as follows. In Sec. II we give a detailed account of the formulation and methods of calculation used in the analysis of the data. First we present the coupled-channel approach and show how to calculate the correlated ΔN wave function in a very efficient way with the Lanczos method. Then we split the inclusive cross section into its various partial cross sections, as there are the contributions of coherent pion production, quasifree Δ decay, and two-nucleon breakup. In Sec. III we discuss the parameters used in our model. We present the results of the cross section calculations and compare them to experimental data [32,33]. Finally, in Sec. IV we give a summary and conclusions.

II. THEORY

We are interested here in the calculation of the inclusive and exclusive cross sections for the ${}^2\text{H}(p,n)$ charge-exchange reaction in the Δ resonance energy region. We consider only forward-scattering angles ($\theta_n \leq 15^\circ$). Since we shall deal with high projectile energies ($T_p = 790$ MeV), we assume that the cross sections can be calculated within the distorted-wave impulse approximation (DWIA). Because of the transparency of the deuteron target it is sufficient to calculate the distortion effects within the eikonal approximation.

A. Inclusive cross section

We start our formulation by writing down the formula for the inclusive ${}^2\text{H}(p,n)$ cross section. Using relativistic kinematics, this cross section is given as

$$d\sigma = \frac{2E_p E_d}{\sqrt{\lambda(s, M_p^2, M_d^2)}} \frac{M_p M_n}{E_p E_n} \frac{d^3 p_n}{(2\pi)^3 2E_n} \times \bar{\sum} (2\pi) \delta(E_p + E_d - E_n - E_f) |T_{fi}|^2. \quad (1)$$

Here the function λ is defined to be $\lambda(s, M_p^2, M_d^2) = [s - (M_p + M_d)^2][s - (M_p - M_d)^2]$ and the indices $p(n)$ and d refer to the proton projectile (neutron ejectile) and the deuteron target, respectively. E_f is the total energy of the final state on the target side, i.e., of all outgoing particles except the neutron ejectile. The c.m. momentum of the final state is fixed by momentum and energy conservation while an integration over the relative momenta has to be performed. In addition, an average over the initial spin orientations and a sum over the final spin orientations of both the projectile and the target spin states are taken. The transition amplitude T_{fi} will be evaluated in the Breit frame (BF) of the target system, where the deuteron state is well described by the usual nonrelativistic wave function.

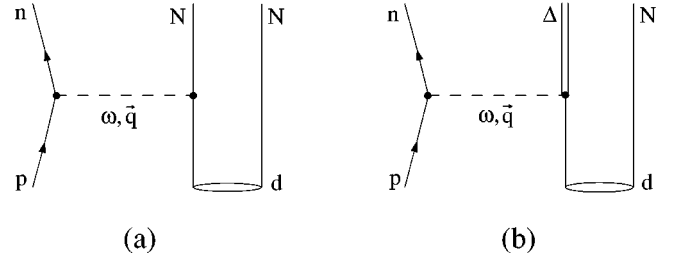


FIG. 1. Impulse approximation diagrams for the ${}^2\text{H}(p,n)$ reaction. Here (a) shows the nucleon excitation and (b) the Δ excitation. (ω, \vec{q}) is the four-momentum transfer to the target. Not shown are exchange diagrams; see the text for details.

Since we want to compare our results with experimental data where the energy and the scattering angle of the outgoing neutron have been measured, we have to calculate the double differential cross section $d^2\sigma/dE_n d\Omega_n$ in the laboratory frame. From Eq. (1) we obtain

$$\left(\frac{d^2\sigma}{dE_n d\Omega_n} \right)^{\text{lab}} = \frac{p_n^{\text{lab}}}{p_n} \left(\frac{d^2\sigma}{dE_n d\Omega_n} \right)^{\text{BF}} = \frac{M_p M_n}{(2\pi)^2} \frac{p_n^{\text{lab}}}{p_p} \frac{E_d}{M_d} \times \bar{\sum} \delta(E_p - E_n + E_d - E_f) |T_{fi}|^2. \quad (2)$$

In the following, cross-section results will always be given in the laboratory system, while every other unlabeled quantity refers to the Breit frame.

B. The uncorrelated source function

In this section we discuss the excitation processes which contribute to ${}^2\text{H}(p,n)$ in impulse approximation. In our model, there are two relevant Feynman diagrams for this case, which are shown in Fig. 1. They represent the nucleon excitation [Fig. 1(a)] and the Δ excitation [Fig. 1(b)] from the deuteron target. The excitation is due to the virtual meson produced by the (p,n) projectile-ejectile system, which is regarded as an external probe. In the first-order DWIA the transition amplitude M_{fi} corresponding to the graphs in Fig. 1 is given as

$$M_{fi} = \sum_{j=1,2} \int d^3 r_0 \phi_n^{(-)*}(\vec{p}_n, \vec{r}_0) \langle \chi_n | \langle \psi_{ab} | \times t_{0j}(\omega, \vec{r}_0 - \vec{r}_j) | \psi_d \rangle | \chi_p \rangle \phi_p^{(+)}(\vec{p}_p, \vec{r}_0). \quad (3)$$

Here \vec{r}_j denotes the coordinates of the projectile ($j=0$) and the target nucleons ($j=1,2$), respectively, which are measured relative to the center of mass of the target. $\phi_p^{(+)}$ and $\phi_n^{(-)*}$ are the distorted-wave functions of projectile and ejectile in the initial and final channels. The spin-isospin part of the projectile (ejectile) wave function is denoted as $|\chi_p\rangle$ ($\langle \chi_n |$). The initial and final states of the target are $|\psi_d\rangle$ and $\langle \psi_{ab} |$, where ab refers to either the NN or the ΔN system. Note that M_{fi} describes only the excitation process, but not the deexcitation, e.g., the free decay of the Δ . Therefore, M_{fi} has to be distinguished from the transition amplitude T_{fi} for the complete reaction.

The t_{0j} in Eq. (3) is the effective interaction between the projectile nucleon 0 and the target nucleon j . A sum over the

two target nucleons has to be performed. The t_{0j} is represented by the free nucleon-nucleon $t_{NN,NN}$ matrix in the case of the nucleon excitation [Fig. 1(a)], while it is approximated by the free $NN \rightarrow N\Delta$ transition operator $t_{NN,N\Delta}$ for the Δ excitation [Fig. 1(b)]. The specific form of these interactions is given in Appendix A. They provide a spin-longitudinal (pionlike) and a spin-transverse (ρ -meson-like) excitation component. The excitation strength parameters are fitted to reproduce the experimental cross section and the spin observables for (p, n) reactions on a nucleon target.

Since the effective t_{0j} is adjusted to experiment, we implicitly account for knockout exchange effects between the projectile and the target nucleons. Note, however, that we neglect the projectile Δ excitation process where the detected neutron comes from the decay of the Δ . For forward neutron angles, the cross section contribution of projectile excitation gives only a small correction to the dominant target excitation process. In Refs. [34,35], the projectile excitation is found to be suppressed by a factor of ≈ 10 in the Δ energy region.

We now take advantage of the fact that at high incident energies and large momentum transfers both interactions t_{0j} turn out to be rather short ranged, i.e., very weakly dependent on the four-momentum transfer $(\omega, \vec{q}) \equiv (E_p - E_n, \vec{p}_p - \vec{p}_n)$. Therefore, they can be well approximated by local operators in r space of essentially δ -function form, that is,

$$t_{0j}(\omega, \vec{r}_0 - \vec{r}_j) = \frac{1}{(2\pi)^3} \int d^3q' \exp[i\vec{q}' \cdot (\vec{r}_0 - \vec{r}_j)] t_{0j}(\omega, \vec{q}') \approx t_{0j}(\omega, \vec{q}) \delta^3(\vec{r}_0 - \vec{r}_j). \quad (4)$$

By inserting Eq. (4) into Eq. (3) we find for the transition amplitude

$$M_{fi} = \langle \psi_{ab} | \hat{\rho} | \psi_d \rangle, \quad (5)$$

where the hadronic transition operator $\hat{\rho}$ is defined as

$$\hat{\rho} = \sum_{j=1,2} \langle \chi_n | t_{0j}(\omega, \vec{q}) X_{DW}(\vec{p}_p, \vec{p}_n, \vec{r}_j) | \chi_p \rangle, \quad (6)$$

with

$$X_{DW}(\vec{p}_p, \vec{p}_n, \vec{r}_j) = \phi_n^*(\vec{p}_n, \vec{r}_j) \phi_p(\vec{p}_p, \vec{r}_j). \quad (7)$$

The product wave function X_{DW} includes the projectile and ejectile distortion effects in the reaction. In the eikonal approximation, Eq. (7) is reduced to $X_{DW}(\vec{q}, \vec{r}_j) = N_{DW}(\vec{q}) \exp(i\vec{q} \cdot \vec{r}_j)$, where $N_{DW}(\vec{q})$ can be calculated from the distorting potential. Thus we get from Eq. (6)

$$\hat{\rho} = N_{DW}(\vec{q}) \langle \chi_n | t_{01}(\omega, \vec{q}) \exp(i\vec{q} \cdot \vec{r}/2) + t_{02}(\omega, \vec{q}) \exp(-i\vec{q} \cdot \vec{r}/2) | \chi_p \rangle, \quad (8)$$

where $\vec{r} = \vec{r}_1 - \vec{r}_2$ is the relative coordinate between the two target nucleons.

Following Ref. [10], we can now introduce source functions for the excitation of either a NN or a ΔN system, respectively, by defining

$$|\rho_N(\vec{r})\rangle = N_{DW}(\vec{q}) \langle \chi_n | t_{01}^{NN,NN}(\omega, \vec{q}) \exp(i\vec{q} \cdot \vec{r}/2) | \chi_p \rangle | \psi_d(\vec{r}) \rangle + (1 \leftrightarrow 2), \quad (9a)$$

$$|\rho_\Delta(\vec{r})\rangle = N_{DW}(\vec{q}) \langle \chi_n | t_{01}^{NN,N\Delta}(\omega, \vec{q}) \exp(i\vec{q} \cdot \vec{r}/2) | \chi_p \rangle | \psi_d(\vec{r}) \rangle + (1 \leftrightarrow 2). \quad (9b)$$

The source functions represent the doorway states excited initially by the external (p, n) charge-exchange field. We call them uncorrelated since they do not include the ‘‘final-state’’ interactions within the excited NN or ΔN system. If the final-state interactions are neglected, the second target nucleon is just a spectator that does not take part in the interaction with the projectile (‘‘spectator approximation’’). The full dynamical treatment of the NN and ΔN systems requires the calculation of correlated continuum wave functions, which we discuss in the next subsection.

C. Inclusion of the ΔN interaction and calculation of the correlated wave function

The inclusion of final state interactions in the description of the ${}^2\text{H}(p, n)$ reaction leads to a coupled-channel problem. In the energy regime considered here, up to four particles appear in the final state because of the pion production. Therefore, the full coupled-channel problem is complicated and can only be solved approximately. In our model we will treat the Δ as a quasiparticle with a given intrinsic decay width and mass. The configuration space \mathcal{H} is build up from NN , ΔN , and πNN sectors, $\mathcal{H} = \mathcal{H}_{NN} \oplus \mathcal{H}_{\Delta N} \oplus \mathcal{H}_{\pi NN}$. The corresponding projection operators are denoted as P_N , P_Δ , and P_Q , respectively, and we will use for any operator Ω the obvious notation $\Omega_{\Delta N} = P_\Delta \Omega P_N$, $\Omega_{Q\Delta} = P_Q \Omega P_\Delta$, etc.

In this formulation the source functions of Eqs. (9a) and (9b) appear to be projections of a unique source function $|\rho\rangle$, i.e.,

$$P_N |\rho\rangle = |\rho_N\rangle, \quad P_\Delta |\rho\rangle = |\rho_\Delta\rangle. \quad (10)$$

Since we restrict ourselves to the DWIA there is no source function for the πNN sector, i.e., $P_Q |\rho\rangle = 0$. We now define the correlated continuum wave function $|\psi\rangle$ as

$$|\psi\rangle = \frac{1}{E - H + i\epsilon} |\rho\rangle = G |\rho\rangle. \quad (11)$$

The Hamiltonian $H = H^0 + V$ contains the free energy H^0 of the system as well as the interaction V . The full propagator G is connected to the unperturbed Greensfunction $G^0 = (E - H^0)^{-1}$ by the equation

$$G = G^0 + G^0 V G. \quad (12)$$

The interaction V introduces the correlation effects into the wave function $|\psi\rangle$. We will demonstrate next how to solve Eq. (11) in a very efficient way by using a few simplifying but physically reasonable approximations.

First we make use of the fact that pion production in intermediate-energy charge-exchange reactions is dominated by the Δ resonance excitation. We assume that $V_{NQ} = V_{QN} = 0$, i.e., there is no direct coupling between the NN and the πNN sector. This means that in our model pion production

proceeds exclusively via an intermediate ΔN system, while the nucleon pole terms are neglected. In the Δ excitation energy regime this approximation should be very good.

The correlated ΔN wave function $|\psi_\Delta\rangle$ follows from Eq. (11) by projecting on the ΔN channel, i.e., $|\psi_\Delta\rangle = P_\Delta|\psi\rangle$. In the Δ energy region, $|\psi_\Delta\rangle$ can be well approximated by

$$|\psi_\Delta\rangle \approx G_{\Delta\Delta}|\rho_\Delta\rangle. \quad (13)$$

Here we neglected the contribution $G_{\Delta N}|\rho_N\rangle$ from the NN source function, which is substantially suppressed in the Δ energy region. The propagator $G_{\Delta\Delta}$ of the ΔN system is determined from Eq. (12), which yields

$$G_{\Delta\Delta} = G_{\Delta\Delta}^0 + G_{\Delta\Delta}^0 V_{\Delta\Delta} G_{\Delta\Delta} + G_{\Delta\Delta}^0 V_{\Delta Q} G_{Q\Delta} + G_{\Delta\Delta}^0 V_{\Delta N} G_{N\Delta}. \quad (14)$$

In this equation, the first and second terms on the right-hand side (rhs) represent the free propagator and the interaction term in the ΔN channel, respectively. The third term $G_{\Delta\Delta}^0 V_{\Delta Q} G_{Q\Delta}$ reflects the emission and reabsorption of pions ($\Delta \rightarrow \pi N \rightarrow \Delta$), which leads to the energy-dependent decay width $\Gamma_\Delta(s_\Delta)$. However, since we treat the Δ as a quasiparticle with an intrinsic width and the physical mass $M_\Delta = 1232$ MeV, this ‘‘self-dressing’’ process is already effectively included in the free propagator $G_{\Delta\Delta}^0$. Therefore, the third term of Eq. (14) has to be dropped. In addition, we also drop the fourth term $G_{\Delta\Delta}^0 V_{\Delta N} G_{N\Delta}$, which generates NN box contributions to the ΔN potential. We do not expect those contributions to influence the ΔN interaction significantly since it seems to be much more likely that the Δ is produced directly in the interaction with the projectile than later on in the final-state interaction of two outgoing nucleons. Hence we are left with

$$G_{\Delta\Delta} \approx G_{\Delta\Delta}^0 + G_{\Delta\Delta}^0 V_{\Delta\Delta} G_{\Delta\Delta} \quad (15)$$

for the ΔN propagator. This approximation has the major advantage that the ΔN channel effectively decouples from the NN channel and therefore can be solved separately.

If we project now Eq. (11) to the possible final channels NN or πNN and make use of Eq. (15), we find

$$P_N|\psi\rangle = G_{NN}|\rho_N\rangle + G_{NN}V_{N\Delta}G_{\Delta\Delta}|\rho_\Delta\rangle, \quad (16a)$$

$$P_Q|\psi\rangle = G_{QQ}V_{Q\Delta}G_{\Delta\Delta}|\rho_\Delta\rangle, \quad (16b)$$

with

$$G_{NN} = G_{NN}^0 + G_{NN}^0 V_{NN} G_{NN}, \quad (17a)$$

$$G_{QQ} = G_\pi^0 \otimes G_{NN}. \quad (17b)$$

Transitions from the ΔN to the NN or πNN channel are accounted for by the corresponding transition potentials $V_{N\Delta}$ and $V_{Q\Delta}$ in Eq. (16). They appear only in first order. The potential V_{NN} in Eq. (17a) describes the NN final-state interaction that includes also ΔN box contributions. We adopt the Paris potential [36,37] for V_{NN} . All effects of the NN potential can be included in the NN wave function $\langle\psi_{NN}|$ for the outgoing nucleons. Furthermore, we assume in Eq. (17b) that the outgoing pion is not distorted from the remaining NN system so that it can be described by a plane wave.

In the remainder of this section, we focus on the ΔN subsystem and the method for solving $|\psi_\Delta\rangle = G_{\Delta\Delta}|\rho_\Delta\rangle$. After having separated the c.m. motion, the full propagator for the relative ΔN wave function is given by

$$G_{\Delta\Delta} = \frac{1}{\epsilon_\Delta + \frac{i}{2}\Gamma_\Delta(s_\Delta) - \hat{T}_\Delta - V_{\Delta\Delta}}, \quad (18)$$

with the excitation energy

$$\epsilon_\Delta = \omega + M - M_\Delta - \frac{(\vec{p}_{\text{cm}})^2}{2(M + M_\Delta)} \quad (19)$$

and the relative kinetic energy

$$\hat{T}_\Delta = \frac{M + M_\Delta}{2MM_\Delta} \vec{p}^2. \quad (20)$$

In the spirit of the model, the propagator contains the energy-dependent width $\Gamma_\Delta(s_\Delta)$ of the Δ resonance. The invariant mass s_Δ is fixed by conservation of four-momentum at the production vertex. For given projectile kinematics we obtain

$$s_\Delta = (M + \omega_{\text{lab}})^2 - \vec{q}_{\text{lab}}^2. \quad (21)$$

Here ω is the energy transfer and \vec{q} the momentum transfer to the deuteron target. Note that the invariant Δ mass is calculated by assuming the target nucleon to be at rest in the laboratory frame (frozen approximation).

In order to solve $|\psi_\Delta\rangle = G_{\Delta\Delta}|\rho_\Delta\rangle$, we transform this equation into an equivalent integral equation [10]

$$|\Lambda_\Delta\rangle = |\rho_\Delta\rangle + V_{\Delta\Delta}G_{\Delta\Delta}^0|\Lambda_\Delta\rangle, \quad (22)$$

so that

$$|\psi_\Delta\rangle = G_{\Delta\Delta}^0|\Lambda_\Delta\rangle. \quad (23)$$

Equation (22) is now reduced to a set of coupled-channel equations for radial wave functions in the following way. First we expand $|\rho_\Delta\rangle$ and $|\Lambda_\Delta\rangle$ in terms of partial waves, i.e.,

$$|\rho_\Delta\rangle = \sum_{S,L,J,M_J} \frac{1}{r} \rho_{SLJM_J}(r) |(SL)JM_J\rangle |11\rangle, \quad (24)$$

$$|\Lambda_\Delta\rangle = \sum_{S,L,J,M_J} \frac{1}{r} \lambda_{SLJM_J}(r) |(SL)JM_J\rangle |11\rangle, \quad (25)$$

where S, L, J, M_J denote the spin, orbital, and total angular momentum quantum numbers of the ΔN system. Due to the special isospin structure of the excitation process, the isospin channel is always $|TM_T\rangle = |11\rangle$. After insertion of Eqs. (24) and (25) into Eq. (22) and projection on $\langle(S'L')J'M'_J|$ we obtain

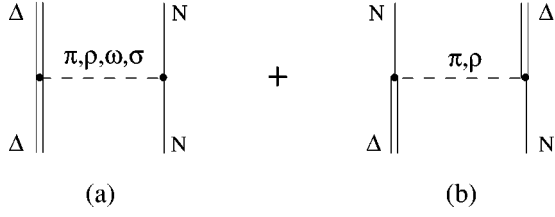


FIG. 2. (a) Direct term and (b) exchange term of the ΔN potential $V_{\Delta\Delta}$. The mesons taken into account are the pion (π), the rho (ρ), the omega (ω), and the sigma (σ).

$$\frac{1}{r}\lambda_n(r) = \frac{1}{r}\rho_n(r) + \sum_{n'} \int dr' r'^2 V_{nn'}(r) G_{\Delta\Delta}^0(r, r') \frac{1}{r'} \lambda_{n'}(r'), \quad (26)$$

where we used the index n as a shorthand notation for $\{SLJM_j\}$. Equation (26) may easily be written as a matrix equation. The radial source functions $\rho_n(r)$ can be calculated in a straightforward manner and are given in Appendix B1. The matrix elements $V_{nn'}(r)$ of the ΔN potential, which is discussed in Sec. III, are given explicitly in Appendix B2. Note that the operation of $G_{\Delta\Delta}^0$ onto $\lambda_{n'}(r')$ involves a radial integration besides the matrix multiplication.

The merit of solving for $|\Lambda_\Delta\rangle$ first lies in the fact that the corresponding radial functions $\lambda_n(r)$ are localized. This fact makes it possible to apply the Lanczos method, which is described in Ref. [10]. It turns out that the Lanczos method allows us to solve Eq. (26) in a very efficient way. Once $|\Lambda_\Delta\rangle$ is known, it is easy to calculate $|\psi_\Delta\rangle$ from Eq. (23) as well.

III. THE MESON-EXCHANGE MODEL FOR THE ΔN INTERACTION

Similar to the NN interaction, the ΔN interaction can be constructed within a meson-exchange model. In the present work we use π , ρ , ω , and σ exchange. While the ω and σ mesons contribute only to the direct term shown in Fig. 2(a), the π and ρ mesons may also induce spin-isospin-flip transitions, which lead to the exchange term of Fig. 2(b). We will discuss the latter term first and start from the interaction Lagrangians $\mathcal{L}_{\pi N\Delta}$ and $\mathcal{L}_{\rho N\Delta}$ given in Ref. [38]. In the non-relativistic reduction we obtain

$$V_{\text{ex}}^\pi(k) = \frac{f_{\pi N\Delta}^2}{m_\pi^2} \vec{T}_1 \cdot \vec{T}_2^\dagger \frac{(\vec{S}_1 \cdot \hat{k})(\vec{S}_2^\dagger \cdot \hat{k})}{k_0^2 - \vec{k}^2 - m_\pi^2 + i\epsilon} + (1 \leftrightarrow 2), \quad (27)$$

$$V_{\text{ex}}^\rho(k) = \frac{f_{\rho N\Delta}^2}{m_\rho^2} \vec{T}_1 \cdot \vec{T}_2^\dagger \frac{(\vec{S}_1 \times \hat{k}) \cdot (\vec{S}_2^\dagger \times \hat{k})}{k_0^2 - \vec{k}^2 - m_\rho^2 + i\epsilon} + (1 \leftrightarrow 2). \quad (28)$$

The corresponding direct interaction terms follow from these potentials by replacing the transition matrices \vec{S}, \vec{S}^\dagger (\vec{T}, \vec{T}^\dagger)

with the spin (isospin) $3/2$ matrix $\vec{\Sigma}$ ($\vec{\Theta}$) and the spin (isospin) $1/2$ matrix $\vec{\sigma}$ ($\vec{\tau}$), respectively. This yields

$$V_{\text{dir}}^\pi(k) = \frac{f_{\pi\Delta\Delta} f_{\pi NN}}{m_\pi^2} \vec{\Theta}_1 \cdot \vec{\tau}_2 \frac{(\vec{\Sigma}_1 \cdot \hat{k})(\vec{\sigma}_2 \cdot \hat{k})}{k_0^2 - \vec{k}^2 - m_\pi^2 + i\epsilon} + (1 \leftrightarrow 2), \quad (29)$$

$$V_{\text{dir}}^\rho(k) = \frac{f_{\rho\Delta\Delta} f_{\rho NN}}{m_\rho^2} \vec{\Theta}_1 \cdot \vec{\tau}_2 \frac{(\vec{\Sigma}_1 \times \hat{k}) \cdot (\vec{\sigma}_2 \times \hat{k})}{k_0^2 - \vec{k}^2 - m_\rho^2 + i\epsilon} + (1 \leftrightarrow 2). \quad (30)$$

For explicit calculation of these potentials we need to know the appropriate coupling constants. The πNN and ρNN couplings are well known experimentally from an analysis of NN scattering data [38]. They may be related to the other couplings by

$$f_{\pi/\rho N\Delta} = 2 f_{\pi/\rho NN}, \quad (31a)$$

$$f_{\pi/\rho\Delta\Delta} = \frac{1}{5} f_{\pi/\rho NN}. \quad (31b)$$

Equation (31b) follows from the static quark model [39]. For Eq. (31a) we decided to use the widely accepted Chew-Low relation [40] instead because the quark model prediction for $f_{\pi N\Delta}$ is too small as compared to the experimental value from the Δ decay.

Additional contributions to the direct part of the ΔN interaction emerge from the ω and σ exchange. We assume the couplings $\omega\Delta\Delta$ and $\sigma\Delta\Delta$ to be the same as for ωNN and σNN , respectively. As before, we choose the nonrelativistic limit of the interaction that follows from $\mathcal{L}_{\omega NN}$ and $\mathcal{L}_{\sigma NN}$ [38]. The resulting potential is

$$V_{\text{dir}}^{\omega+\sigma}(k) = +g_{\omega\Delta\Delta} g_{\omega NN} \frac{1}{k_0^2 - \vec{k}^2 - m_\omega^2 + i\epsilon} - g_{\sigma\Delta\Delta} g_{\sigma NN} \frac{1}{k_0^2 - \vec{k}^2 - m_\sigma^2 + i\epsilon}. \quad (32)$$

The full potential for the ΔN interaction is the sum of the different contributions from Eqs. (27)–(30) and (32); hence

$$V_{\Delta\Delta}(k) = V_{\text{ex}}^{\pi+\rho}(k) + V_{\text{dir}}^{\pi+\rho}(k) + V_{\text{dir}}^{\omega+\sigma}(k). \quad (33)$$

Note that the $\pi(\rho)$ contribution covers the LO(TR) spin-isospin part of the potential, while the $\omega + \sigma$ contribution is spin-isospin independent. Furthermore, we point out that we use monopole form factors of the type

$$F(k^2) = \left(\frac{\Lambda^2 - m^2}{\Lambda^2 - k_0^2 + \vec{k}^2} \right) \quad (34)$$

at all vertices. In the formulas given here, the form factors are always suppressed in order to simplify the notation.

Since the ΔN potential is required in r space, a Fourier transformation of $V_{\Delta\Delta}(k)$ has to be performed. This involves an integration over all possible three momentum transfers \vec{k} .

TABLE I. Parameters used in the meson exchange model for the ΔN interaction.

Meson	$f_{\alpha NN}^2/4\pi$	$f_{\alpha N\Delta}^2/4\pi$	$f_{\alpha\Delta\Delta}^2/4\pi$	Λ_α (GeV)	m_α (MeV)
π	0.08	0.32	0.0032	1.1	138
ρ	5.4	21.6	0.216	1.4	770
ω	8.1 ^a		8.1 ^a	1.7	783
σ	5.7 ^a		5.7 ^a	1.4	570

^a $g_{\alpha NN}^2/4\pi$ and $g_{\alpha\Delta\Delta}^2/4\pi$ are given, respectively.

On the other hand, the energy transfer k_0 is a free parameter that has to be fixed within the kinematic allowed region. Because the Δ resonance is assumed to keep its invariant mass during the propagation, we choose $k_0=0$ in the direct interaction terms and $k_0=\omega$ in the exchange terms. This choice makes the potential energy dependent, as it should be.

The $\Delta N \rightarrow NN$ transition potential $V_{N\Delta}$ is constructed in complete analogy from Eqs. (27) and (28) by replacing $S^\dagger(T^\dagger)$ with $\vec{\sigma}(\vec{\tau})$. Of course, only the π and the ρ meson contribute to $V_{N\Delta}$. For the energy transfer in this case, we adopt the choice $k_0=\omega/2$ of Ref. [17]. As far as the spin-longitudinal part of $V_{N\Delta}$ is concerned, we use an additional zero-range interaction

$$V_{N\Delta}^\delta(k) = g_{N\Delta} \frac{f_{\pi N\Delta} f_{\pi NN}}{m_\pi^2} \vec{T}_1 \cdot \vec{\tau}_2 (\vec{S}_1 \cdot \hat{k}) (\vec{\sigma}_2^\dagger \cdot \hat{k}), \quad (35)$$

with the Landau-Migdal parameter $g_{N\Delta}=1/3$ [10]. This additional contribution cancels the nonphysical zero-range part of the π -exchange potential. In principle, one should introduce a corresponding Landau-Migdal term for $V_{\Delta\Delta}$ with a strength parameter $g_{\Delta\Delta}$ as well. However, due to the presence of not only exchange but also direct contributions to the potential, the zero-range parts cancel anyway and $g_{\Delta\Delta}$ turns out to have no influence on the results. Therefore, we decided to do without and chose $g_{\Delta\Delta}=0$.

In Table I an overview of all the meson parameters used for the ΔN potentials is given. We made sure that with these parameters, our model consistently reproduces experimental results for pion absorption on the deuteron, $\pi^+ + d \rightarrow 2p$ [41].

IV. DECOMPOSITION OF THE INCLUSIVE CROSS SECTION

We will now decompose the inclusive ${}^2\text{H}(p,n)$ cross section into partial cross sections corresponding to different physical processes. These processes are schematically represented by the diagrams of Figs. 3(a)–3(d). We distinguish between quasielastic scattering [Fig. 3(a)], p -wave rescattering [Fig. 3(b)], coherent pion production [Fig. 3(c)], and quasifree Δ decay [Fig. 3(d)]. For each process, only the lowest-order diagram is shown, but not the higher-order diagrams, which are nevertheless accounted for in the calculation. Also not shown are the exchange diagrams discussed in Sec. II B.

Quasielastic scattering and p -wave rescattering both result in a two-proton ($2p$) final state on the target side. Their transition amplitudes interfere coherently with each other. While the quasielastic scattering directly leads to the $2p$ system, the p -wave rescattering contribution involves an intermediate ΔN state and arises due to the $\Delta N \rightarrow NN$ transition

potential $V_{N\Delta}$; see Figs. 3(a) and 3(b). Since in both cases the deuteron is simply broken up into two protons, we will refer to this reaction channel as to the breakup channel (BU).

At higher energy transfers, the πNN final channel is the most important one. We remind the reader that we assume the pion production to proceed always through Δ resonance excitation. If the two nucleons in the final state form a bound deuteron state, we speak of coherent pion production (CP); see Fig. 3(c). In this case, the outgoing pion is naturally a π^+ . On the other hand, if the two outgoing nucleons are unbound, we speak of quasifree Δ decay or quasifree pion production (QF); see Fig. 3(d). There are two possible final isospin configurations for this process, namely, $\pi^+ np$ and $\pi^0 pp$. We remark that the expressions ‘‘quasifree’’ and ‘‘coherent’’ used here for the different pion production modes are chosen in conformity with Ref. [10]. They just shall distinguish between the two πNN final channels by indicating whether the deuteron is broken up (quasifree) or not (coherent).

According to these different reaction mechanisms, the inclusive cross section of Eq. (2) may now be split into its various components. We express the squared transition matrix as the sum,

$$\sum \delta(\omega + E_d - E_f) |T_{fi}|^2 = \frac{1}{6} (S_{\text{BU}} + S_{\text{CP}} + S_{\text{QF}}). \quad (36)$$

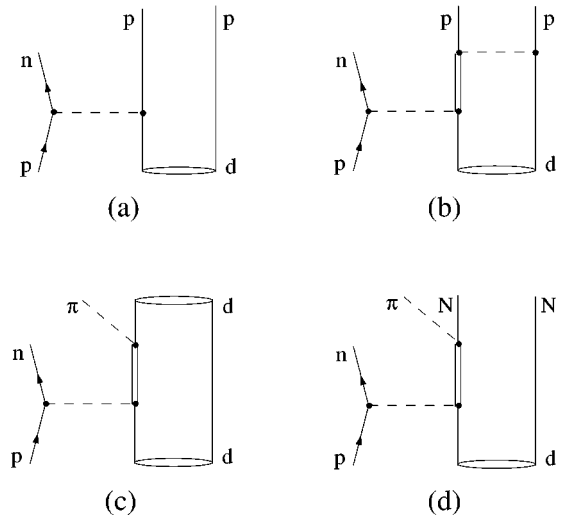


FIG. 3. Reaction mechanisms of the different contributions to the inclusive cross section in our analysis. Only the lowest-order diagrams are shown. They represent (a) quasielastic scattering, (b) p -wave rescattering, (c) coherent pion production, and (d) quasifree Δ decay.

Here the strength functions S implicitly include the integration over free relative momenta as well as the summation over all spin configurations and the factor $\frac{1}{6}$ arises from the average over the initial spin configurations.

Using Eq. (16a), the strength function for the deuteron breakup channel BU is found to be

$$S_{\text{BU}} = \sum_{S_i, S_f} \int \frac{d^3p}{(2\pi)^3} \delta(\omega + E_d - E_{2p}) |\langle \psi_{NN} | \rho_N \rangle + \langle \psi_{NN} | V_{N\Delta} | \psi_\Delta \rangle|^2. \quad (37)$$

The first matrix element in the sum of the rhs describes the quasielastic scattering, and the second matrix element describes the p -wave rescattering. \vec{p} denotes the relative momentum of the two outgoing protons. Their final-state interaction V_{NN} is included in $\langle \psi_{NN} |$, while the correlated source function $|\psi_\Delta\rangle$ accounts for the ΔN interaction $V_{\Delta\Delta}$.

In order to calculate the matrix element for coherent pion production, we define the operator

$$\hat{f}_\pi = e^{-i\vec{q}_\pi \cdot \vec{r}/2} \frac{f_{\pi N\Delta}}{m_\pi} T_{1\nu} \vec{S}_1 \cdot \vec{\kappa}_\pi + (1 \leftrightarrow 2), \quad (38)$$

where $\vec{\kappa}_\pi$ is the relative pion-nucleon momentum in the Δ rest frame. The operator describes the decay of the Δ into a real pion and a nucleon and contains also the plane wave of the outgoing pion. Applying \hat{f}_π to the ΔN wave function and projecting onto the final deuteron state yields

$$S_{\text{CP}} = \sum_{S_i, S_f} \int \frac{d^3q_\pi}{(2\pi)^3 2E_\pi} \delta(\omega + E_d - E_\pi - E'_d) |\langle \psi_d | \hat{f}_\pi | \psi_\Delta \rangle|^2 \quad (39)$$

for the CP strength function. Equation (39) may also be rewritten as

$$S_{\text{CP}} = \sum_{S_i} \left\langle \psi_\Delta \left| \frac{1}{\pi} \text{Im}(V_{\Delta\Delta}) \right| \psi_\Delta \right\rangle, \quad (40)$$

where we used the fact that $E_d \approx E'_d$ holds in the Breit frame. Hence the coherent pion production amplitude is directly connected to the imaginary part of the ΔN interaction. We remark that this is true only if $\text{Im}(V_{\Delta\Delta})$ comes exclusively from the π exchange interaction, as it is the case in the Δ energy region.

From Eq. (39) we may easily calculate the angular distribution of the coherent pions, namely, the triple differential cross section $d^3\sigma_{\text{CP}}/dE_n d\Omega_n d\Omega_\pi$, by omitting the integration over the pion momentum. The result is

$$\left(\frac{d^3\sigma_{\text{CP}}}{dE_n d\Omega_n d\Omega_\pi} \right)^{\text{lab}} = \frac{M_p M_n p_n^{\text{lab}} E_d q_\pi^2}{(2\pi)^5 p_p^{\text{lab}} M_d 2E_\pi} \times \frac{dq_\pi}{dE_f} |\langle \psi_d | \hat{f}_\pi | \psi_\Delta \rangle|^2, \quad (41)$$

with the same notation for the phase space factor as in Eq. (2).

In analogy to Eq. (40), the pion production from quasifree Δ decay is ascribed to the imaginary part of the Δ self-

dressing, i.e., to the intrinsic Δ decay width. As a consequence, the QF strength function is given as

$$S_{\text{QF}} = \sum_{S_i} \left\langle \psi_\Delta \left| \frac{1}{\pi} \frac{\Gamma_\Delta(s_\Delta)}{2} \right| \psi_\Delta \right\rangle. \quad (42)$$

The differential QF cross section could also be calculated from the matrix element $|\langle \psi_{NN} | \hat{f}_\pi | \psi_\Delta \rangle|^2$. Equation (42) would then be recovered after integration over the pion momentum, as in Eq. (39), and over the relative NN momentum as well.

To summarize we have decomposed the inclusive ${}^2\text{H}(p, n)$ cross section into three parts: the quasifree Δ decay, the coherent pion production, and the two-nucleon breakup of the deuteron (which is equal to the quasielastic plus p -wave rescattering). Of course there are other possible contributions to the inclusive cross section, but in the energy region under consideration, they should be less important than the ones mentioned and are therefore neglected in the present paper.

V. RESULTS AND DISCUSSION

A. Input parameters

With the formalism described in the previous sections, we have calculated energy spectra at various scattering angles θ_n for the ${}^2\text{H}(p, n)$ reaction at $T_p = 790$ MeV. The deuteron wave function and the two-nucleon wave function were generated from the Paris potential [36,37]. A constant distortion factor of $N_{DW}^2 = 0.9$ was applied [42,34]. For the ΔN potential we used coupling constants and cutoff parameters as given in Table I. The free Δ mass is $M_\Delta = 1232$ MeV and the free decay width $\Gamma_\Delta(s_\Delta)$ was parametrized in the usual form [43].

The strength parameters in the effective parametrizations of $t_{NN, NN}$ and $t_{NN, N\Delta}$ (cf. Sec. II B and Appendix A) have been fitted to reproduce experimental results for the nucleon target. In order to demonstrate the quality of this fit, we present in Fig. 4 results for the ${}^1\text{H}(p, n)\Delta^{++}$ cross section at $T_p = 790$ MeV. The theoretical calculations are compared with the experimental data [32] at various scattering angles θ_n of the outgoing neutron. Both the shape and magnitude are reproduced very well. We remark that also the LO/TR ratio of 1/2 used in the parametrization of $t_{NN, N\Delta}$ has been observed experimentally [44,45].

B. Inclusive spectra of the ${}^2\text{H}(p, n)$ reaction

In Fig. 5 we show the calculated inclusive cross section for the $\theta_n = 0^\circ$ spectrum of the ${}^2\text{H}(p, n)$ reaction in comparison with the experimental data [32]. The different contributions to the inclusive cross section are also shown separately. The possible reaction channels are the quasifree Δ decay, the coherent pion production, and the deuteron breakup due to quasielastic scattering and p -wave rescattering.

At energies $\omega_{\text{lab}} \leq 50$, the spectrum exhibits a prominent peak that arises dominantly from quasielastic scattering. The small width of the peak reflects the Fermi motion of the nucleons in the deuteron target. The peak is described well by our calculations.

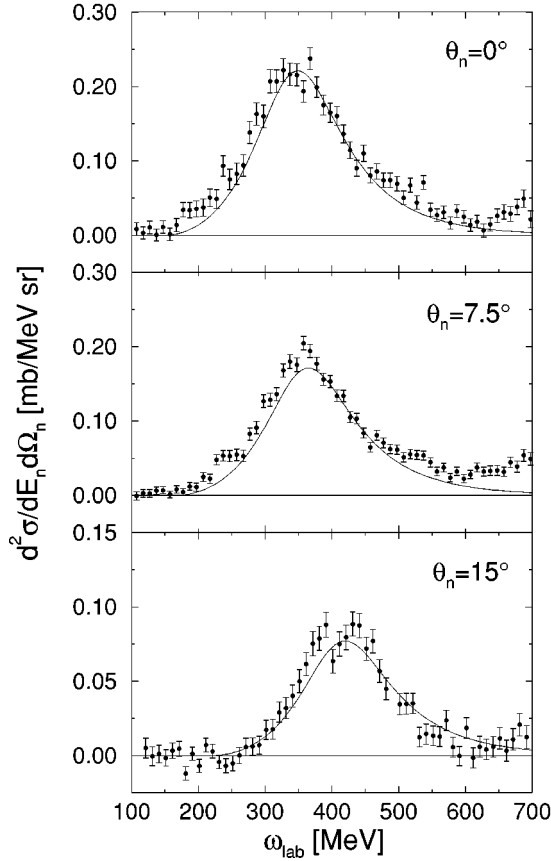


FIG. 4. Differential cross section for the reaction ${}^1\text{H}(p,n)\Delta^{++}$ at $T_p=790$ MeV and at scattering angles $\theta_n=0^\circ$, 7.5° , and 15° , respectively. The theoretical calculation uses the parametrization of $t_{NN,\Delta}$ as given in Appendix A. Experimental data are from Ref. [32].

In the energy region of the Δ resonance peak position at $\omega_{\text{lab}}=340$ MeV, the theoretical result is also in good agreement with the data. The cross section in this region is mainly due to the quasifree decay of the Δ . The cross-section con-

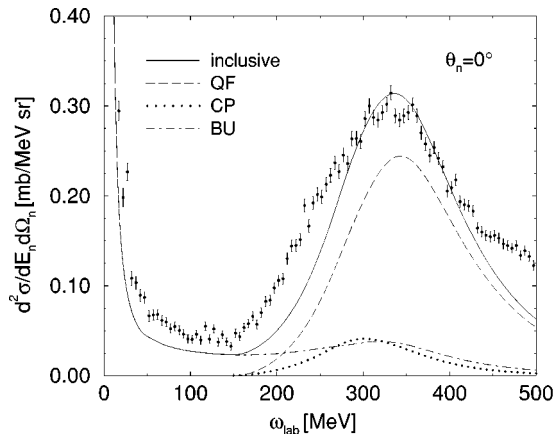


FIG. 5. Zero-degree neutron spectrum for the reaction ${}^2\text{H}(p,n)$ at $T_p=790$ MeV. The theoretical calculation (solid line) includes contributions from quasifree Δ decay (QF, dashed line), coherent pion production (CP, dotted line), and two-nucleon breakup of the deuteron (BU, dash-dotted line). Experimental data are from Ref. [32].

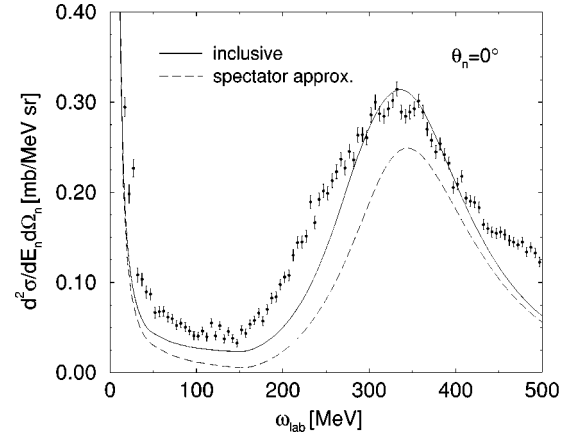


FIG. 6. Full calculation with inclusion of baryonic exchange currents (solid line) in comparison with the ‘‘spectator approximation’’ result where $V_{\Delta\Delta}=V_{N\Delta}=0$ (dashed line). Experimental data are from Ref. [32].

tribution due to coherent pion production is by a factor of ≈ 5 smaller than the QF contribution.

At high-energy transfers $\omega_{\text{lab}} \geq 450$ MeV, our calculation underestimates the experimental cross section. The missing cross section can be ascribed to the excitation of higher nucleon resonances, e.g., $N^*(1440)$. Those configurations are not included in our model space and therefore the underestimate of the cross section is not surprising.

The theoretical calculations also underestimate the data in the so-called dip region between the quasielastic peak and the Δ peak, i.e., in the energy region $50 \text{ MeV} \leq \omega_{\text{lab}} \leq 250$ MeV. The experimental cross section here is believed to result mainly from two-body exchange currents in the target. Only the baryonic exchange currents connected with the Δ are accounted for in our calculations. They are included in the ΔN interaction $V_{\Delta\Delta}$ and in the transition potential $V_{N\Delta}$, which gives rise to the p -wave rescattering contribution. In Fig. 6 our full model calculation is compared with a calculation obtained within the ‘‘spectator approximation.’’ The latter corresponds to the case $V_{\Delta\Delta}=V_{N\Delta}=0$. It can be seen that the inclusion of the exchange currents significantly improves the theoretical description of the experimental data. Nevertheless, we still underestimate the cross section in the dip region by a factor of about 1.5. This is most probably due to the neglect of purely mesonic exchange currents, e.g., the s -wave rescattering of pions. At the low-energy side of the Δ peak, additional contributions from projectile Δ excitation could be important as well. They are expected to be very small at the Δ peak position, but getting larger as the energy transfer decreases [35]. On the other hand, there may also be a need for relativistic corrections in the dynamical treatment of the ΔN system.

In the following we shall demonstrate that almost all of the cross section in the dip region is spin transversal, while the spin-longitudinal cross section is relatively small. This statement can be tested by measuring spin observables that allow for a separation of the inclusive cross section into its LO and TR components [33]. This separation is shown in Fig. 7 together with the theoretical results. The measured LO cross section is reproduced very well by our calculation. On

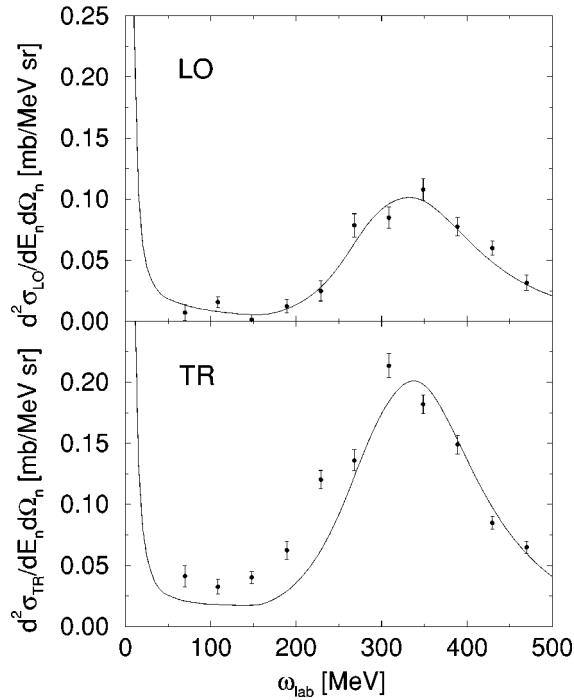


FIG. 7. Separation of the inclusive cross section into spin-longitudinal (LO, $\sim \vec{\sigma} \cdot \hat{q}$) and spin-transverse components (TR, $\sim \vec{\sigma} \times \hat{q}$). Experimental data are from Ref. [33].

the other hand, the measured TR cross section is both shifted and enhanced with respect to the calculation. This apparent shift clearly indicates that our calculations produce not enough TR cross section in the dip region. A similar effect is observed in inelastic electron scattering off nuclei [46,47]. In the (e, e') reactions, the virtual photon also probes the TR response of the target. In scattering off nuclei, the experimental (e, e') cross section in the dip region is considerably larger than expected. The additional cross section cannot be explained by one-body currents and has to be ascribed to two-body currents [48]. Such rescattering effects have also proven to be quite important for coherent pion photoproduction on the deuteron [21]. In hadronic interactions, the ρ meson should take over the role of the photon. In a recent paper of Lee [49], the author found indeed a large contribution to the ${}^2\text{H}(p, n)$ inclusive cross section from the exchange of a ρ meson that couples to a ‘‘pion in flight’’ in the deuteron. We could not reproduce this result. Since there are many other possible meson exchange currents that have not been considered for the ${}^2\text{H}(p, n)$ reaction so far, the dip-region puzzle remains a problem to be solved.

The theoretical description of the experimental ${}^2\text{H}(p, n)$ spectra at higher scattering angles is of the same quality as for zero-degree scattering. This can be seen from Fig. 8, where we compare the theoretical ${}^2\text{H}(p, n)$ cross section with data at $\theta_n = 7.5^\circ$ and $\theta_n = 15^\circ$, respectively. At the low-energy side of the Δ , the theoretical curves show again a characteristic underestimate of the data. Apart from this effect both the shape and the magnitude of the spectra are described well. Our calculations correctly reproduce the change of the quasielastic and the Δ peak position with the scattering angle.

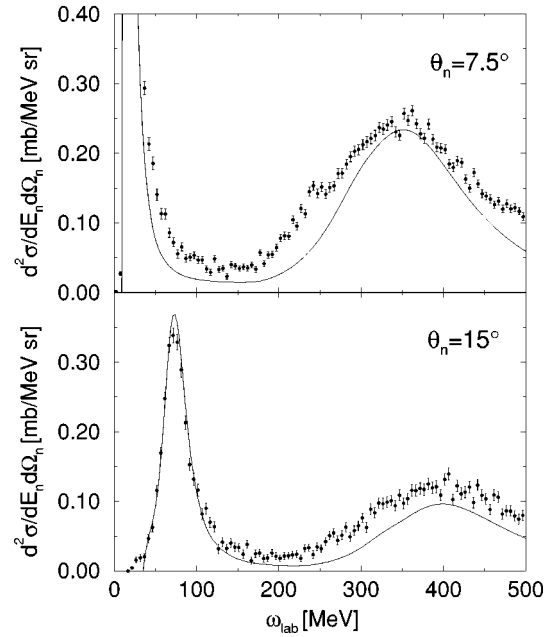


FIG. 8. Neutron spectra for the reaction ${}^2\text{H}(p, n)$ at $T_p = 790$ MeV at scattering angles of $\theta_n = 7.5^\circ$ and $\theta_n = 15^\circ$, respectively. Experimental data are from Ref. [32].

C. Influence of the ΔN interaction on the exclusive spectra

We now discuss the influence of the ΔN interaction on the three partial contributions (QF, CP, and BU) to the cross section. As we will demonstrate, the coherent pion production is most sensitive to $V_{\Delta\Delta}$. This sensitivity is a combined effect of the attractive pion exchange, the spin-longitudinal $\pi N\Delta$ coupling, and the structure of the deuteron wave function. In the following discussion we will focus on the exclusive ${}^2\text{H}(p, n\pi^+){}^2\text{H}$ spectra first.

In Fig. 9 theoretical results for the exclusive ${}^2\text{H}(p, n\pi^+){}^2\text{H}$ cross section are shown. The calculation without inclusion of the ΔN interaction (i.e., $V_{\Delta\Delta} = 0$)

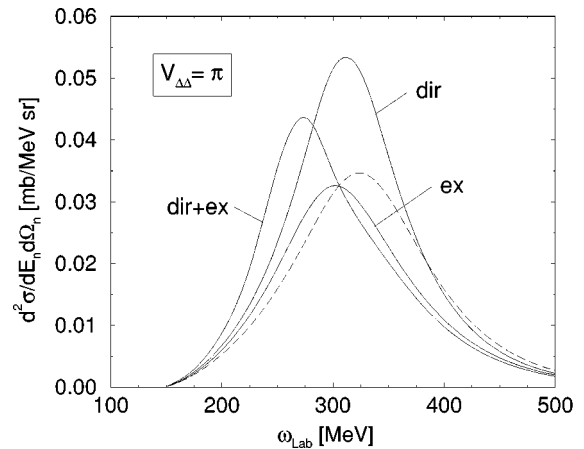


FIG. 9. Effects on coherent pion production ${}^2\text{H}(p, n\pi^+){}^2\text{H}$ resulting from the direct (dir) and the exchange (ex) contribution of the π meson to $V_{\Delta\Delta}$ (solid lines). The line labeled dir+ex shows the sum of direct and exchange contributions of the π . Note the apparent shift compared to the dashed line, which represents the spectator approximation $V_{\Delta\Delta} = 0$.

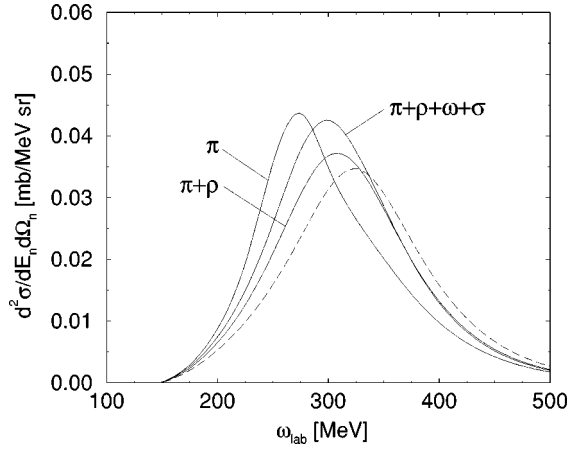


FIG. 10. Effects on coherent pion production ${}^2\text{H}(p,n\pi^+){}^2\text{H}$ resulting from the π , ρ , ω , and σ meson contributions to $V_{\Delta\Delta}$ (solid lines). The line labeled $\pi+\rho+\omega+\sigma$ represents the full model calculation. The dashed line shows the spectator approximation $V_{\Delta\Delta}=0$.

compared with a calculation where only the π -meson contribution to $V_{\Delta\Delta}$ was taken into account. The effects of the direct and the exchange part of the π -mediated interaction are also examined separately. Obviously both parts are of equal importance, which may be surprising at first. It is true that because of the smallness of the $\pi\Delta\Delta$ coupling constant, the direct part should be suppressed by a factor of ≈ 20 compared to the exchange part, but in the $T=1$ channel of the ΔN system that is relevant here the spin-isospin matrix elements turn out to be larger by approximately the same amount. Therefore, it is essential to include both the direct and the exchange contribution in the ΔN interaction. In the case of the π exchange, the interference effect of both contributions leads to a very strong attraction between the Δ and the second target nucleon. The result is a shift of the cross-section peak position downward in energy (by ≈ 60 MeV; cf. Fig. 9). Most of the attraction is caused by the tensor part of the π , whereas the central part is less important for the peak position but influences the overall magnitude of the result.

By including not only the π but also the ρ , ω , and σ mesons in $V_{\Delta\Delta}$, we obtain the results presented in Fig. 10. It can be seen that both the peak position and the magnitude of the exclusive ${}^2\text{H}(p,n\pi^+){}^2\text{H}$ cross section depend quite sensitively on the specific form of the ΔN potential. In comparison to the result with only π exchange, the inclusion of π and ρ in the ΔN interaction leads to a less attractive potential and hence to a smaller shift of the peak position. The reason for this behavior is the partial cancellation of the π and ρ tensor forces, which have opposite sign. For the direct part of the interaction, the ω and the σ meson cause an additional short-range repulsion and a medium-range attraction, respectively, which leads to an additional enhancement of the cross section. The final result for the ${}^2\text{H}(p,n\pi^+){}^2\text{H}$ spectrum (i.e., the result with inclusion of $\pi+\rho+\omega+\sigma$ in $V_{\Delta\Delta}$) is quite different from the spectator approximation (i.e., the result with $V_{\Delta\Delta}=0$). Most remarkable is the shift of the peak position downward in energy by about 30 MeV. As discussed above, the main reason for this shift is the attractive pion

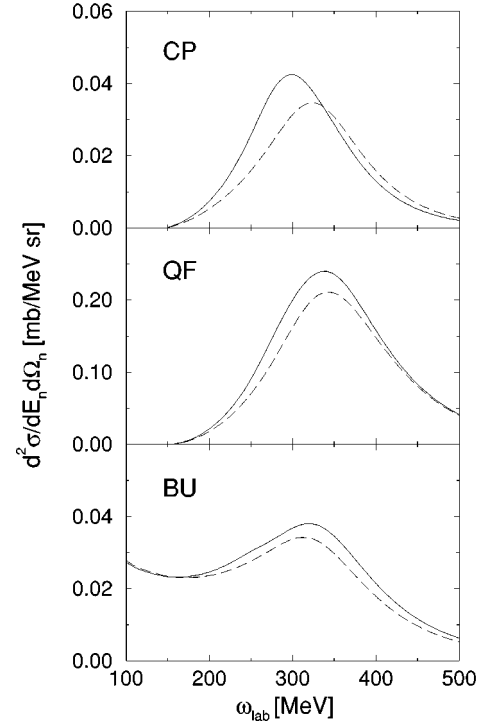


FIG. 11. Effect of $V_{\Delta\Delta}$ on the exclusive cross section for coherent pion production (CP), quasifree Δ decay (QF), and deuteron breakup (BU). Calculations with (solid lines) and without (dashed lines) $V_{\Delta\Delta}$. Note the different scalings of the vertical axis.

exchange, i.e., the attractive LO part of the ΔN potential. The amount of the peak shift is directly related to the interaction strength of $V_{\Delta\Delta}$.

This result attracts further interest because there is no comparable peak shift due to $V_{\Delta\Delta}$ for the quasifree Δ decay cross section and also not for the deuteron breakup. Figure 11 shows the results with and without inclusion of $V_{\Delta\Delta}$ for the coherent pion production, the quasifree Δ decay, and the deuteron breakup. In both the QF and the BU channel, the cross section is slightly enlarged and broadened due to the ΔN interaction, but there is no significant shift of the peak position.

In order to understand this different behavior, we perform a multipole decomposition of the partial cross sections and split them into two contributions corresponding to unnatural parity (UP) states ($J^P=0^-,1^+,2^-, \dots$) of the ΔN system and to natural parity (NP) states ($J^P=1^-,2^+, \dots$), respectively. For the three reaction channels under consideration, this decomposition is shown in Fig. 12. For each case, the full calculation is compared with the spectator approximation. One recognizes that the cross-section contributions of the UP states are always lowered in excitation energy by the ΔN interaction, while the NP states are not. This is explained by the fact that there is a strong coupling of the pion to the UP (pionlike) states but just a weak coupling to the NP states. Therefore, only the UP states are substantially influenced by the attraction of the LO part of $V_{\Delta\Delta}$. For the coherent pion production, the spectrum is clearly dominated by the UP states. This is an effect of the LO spin structure of the deexcitation process and of the deuteron wave function (which

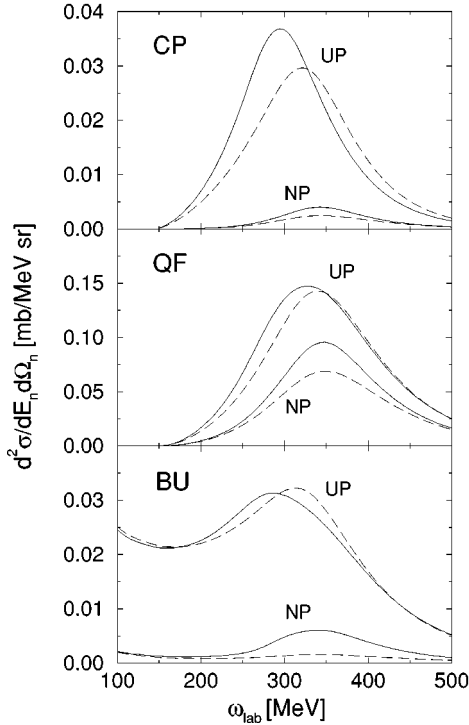


FIG. 12. Decomposition of the exclusive cross sections into contributions from unnatural parity states (UP) and natural parity states (NP). Calculations with (solid lines) and without (dashed lines) $V_{\Delta\Delta}$. Note the different scalings of the vertical axis.

selects spin $S=1$ and orbital momentum $L=(0,2)$ in the final state.

For the quasifree Δ decay, the final deuteron state is replaced by a final unbound NN state. Since the two outgoing nucleons are free, we have no particular spin selection rule in the deexcitation process for this case and thus all partial waves can contribute. As can be seen from Fig. 12, the NP states become more important for the QF decay and the overall energy shift more or less disappears. For the $2p$ breakup, the $\Delta N \rightarrow NN$ transition potential $V_{N\Delta}$ provides not only a LO but also a TR component. The energy shift of the UP states is compensated by a relative large enhancement of the NP states, which results from TR excitation. Moreover, the p -wave rescattering interferes with the quasielastic scattering that has no intermediate ΔN configuration; hence the effects of $V_{\Delta\Delta}$ are partially smeared out.

To complete the discussion about the influence of the ΔN interaction, we show in Fig. 13 the contributions of three characteristic ΔN partial waves to the exclusive ${}^2\text{H}(p, n\pi^+){}^2\text{H}$ cross section. All selected partial waves have unnatural parity and therefore couple strongly to the pion. The spectrum is absolutely dominated by the 5S_2 partial wave of the ΔN system. Because the Δ and the nucleon have relative angular momentum zero in this case, there is no centrifugal barrier in the potential and the attraction becomes largest. That accounts for the strong energy shift in this partial wave. The partial waves with higher angular momentum $L \geq 1$ are subjected to a less attractive potential due to the centrifugal barrier and therefore do not exhibit such a lowering in the excitation energy. As can be seen from Fig. 13, the 5P_3 partial wave is only enhanced but not shifted due to $V_{\Delta\Delta}$. For the 5D_0 partial wave, the potential has a minor

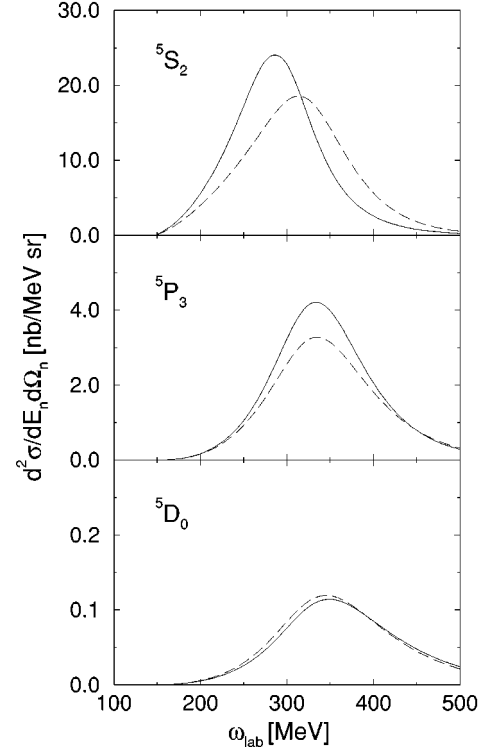


FIG. 13. Multipole decomposition of the zero-degree spectrum for the exclusive ${}^2\text{H}(p, n\pi^+){}^2\text{H}$ reaction. Calculations with (solid lines) and without (dashed lines) $V_{\Delta\Delta}$ for three characteristic partial waves of the ΔN system are shown. Note the different scalings of the vertical axis.

effect and even gets repulsive. Compared to 5S_2 , the higher partial waves are by far less important, which results in the surviving of the downward energy shift in the full spectrum.

We conclude that neither the QF nor the BU process shows the same sensitivity to the LO channel as the CP process. Therefore, only the exclusive ${}^2\text{H}(p, n\pi^+){}^2\text{H}$ spectrum clearly exhibits a lowering of the Δ excitation energy. This fact makes the coherent pion production most suitable to examine the effects of the ΔN interaction.

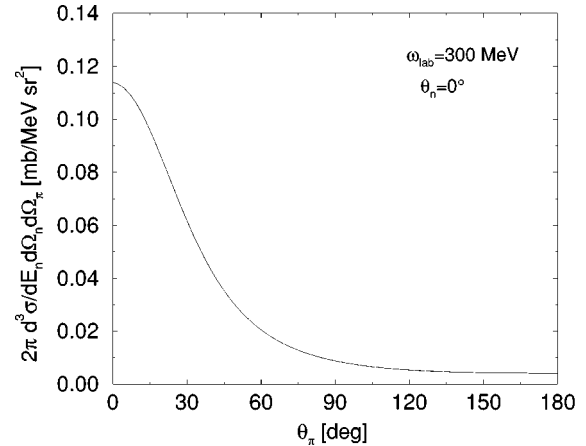


FIG. 14. Triple differential cross section for the ${}^2\text{H}(p, n\pi^+){}^2\text{H}$ reaction at $\omega_{\text{lab}}=300$ MeV and $\theta_n=0^\circ$. The cross section is shown as a function of θ_π , which is the angle between the outgoing π^+ and the momentum transfer \vec{q} on the deuteron target.

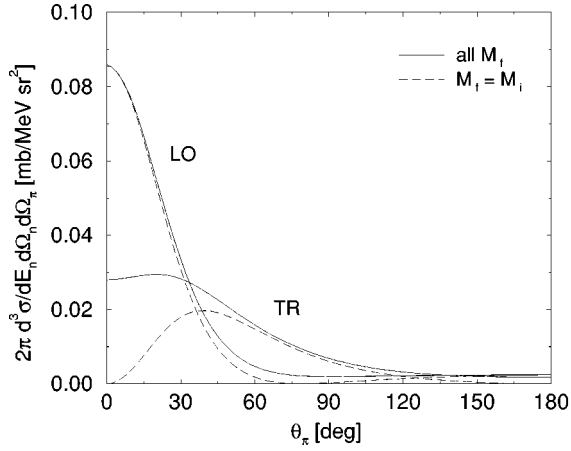


FIG. 15. Triple differential cross section for the ${}^2\text{H}(p, n \pi^+){}^2\text{H}$ reaction in the spin-longitudinal (LO) and the spin-transversal (TR) channel. $M_i(M_f)$ refers to the spin projection of the deuteron in the initial (final) state, hence the dashed curves labeled $M_i = M_f$ show a calculation where spin flips of the deuteron have been excluded.

D. Exclusive differential cross section for coherent pion production

In this section we present our results for the angular distribution of the coherently produced pions. In Fig. 14 the triple differential cross section $d^3\sigma/dE_n d\Omega_n d\Omega_\pi$ of the exclusive ${}^2\text{H}(p, n \pi^+){}^2\text{H}$ reaction is plotted as a function of θ_π which is the angle between the outgoing π^+ and the three-momentum transfer \vec{q} . The energy transfer was chosen to be $\omega_{\text{lab}} = 300$ MeV and the neutron scattering angle is $\theta_n = 0^\circ$. One recognizes that the angular distribution is strongly forward peaked. This means that most of the coherent pions are emitted into the direction of the three-momentum transfer.

The contributions of the spin-longitudinal and the spin-transverse channel to the differential cross section are shown separately in Fig. 15. One can understand some of the main features of these angular distributions by analyzing the spin structure of the transition operators.

For the LO channel, the product of the deexcitation and excitation operators turns out to be

$$(\vec{S} \cdot \vec{p}_\pi)(\vec{S}^\dagger \cdot \vec{q}) = \frac{2}{3} \vec{p}_\pi \cdot \vec{q} - \frac{i}{3} \vec{\sigma} \cdot (\vec{p}_\pi \times \vec{q}). \quad (43)$$

The first term on the rhs of Eq. (43) gives rise to a factor $q p_\pi \cos \theta_\pi$ in the transition amplitude and thus to a factor $\cos^2 \theta_\pi$ in the cross section. This factor has a maximum at $\theta_\pi = 0^\circ$ and thus partially explains the strongly forward-peaked LO contribution in Fig. 15. There are, however, additional angular-dependent factors such as the kinematic phase-space factor and the overlap integral with the outgoing pion wave in Eq. (39). Those factors become larger as θ_π gets smaller and therefore pronounce the forward peaking of the angular distribution even more. All reaction events where the spin of the deuteron is flipped are produced by the second term on the rhs of Eq. (43). At small scattering angles this cross-section contribution is proportional to $\sin^2 \theta_\pi$ and thus vanishes at $\theta_\pi = 0^\circ$.

We would like to mention that the angular distribution of the LO component is very similar to that of the pion elastic scattering [14,21]. In fact, one may view the coherent pion

production as a kind of elastic-scattering process, in which an initially off-mass-shell pion with the momentum \vec{q} is converted into an on-mass-shell pion by the multiple scattering in the deuteron. This conversion process is possible because the deuteron as a whole can provide the extra recoil momentum needed to put the pion on its mass shell.

For the TR channel, the deexcitation and excitation operators yield a spin structure

$$(\vec{S} \cdot \vec{p}_\pi)(\vec{S}^\dagger \times \vec{q}) = \frac{2}{3} \vec{p}_\pi \times \vec{q} - \frac{i}{3} (\vec{\sigma} \times \vec{p}_\pi) \times \vec{q}. \quad (44)$$

As before, the first term on the rhs of Eq. (44) is connected with non-spin-flip events, while the second term induces spin flips of the deuteron. The angular distribution of the non-spin-flip part is proportional to $|\vec{p}_\pi \times \vec{q}|^2 = (p_\pi q \sin \theta_\pi)^2$. This factor vanishes for $\theta_\pi = 0^\circ$ and peaks for $\theta_\pi = 90^\circ$. The additional angular dependent factors as discussed before lead to a more-forward-peaked distribution. As can be seen from Fig. 15, the TR non-spin-flip component has its maximum at about $\theta_\pi \approx 40^\circ$ and is zero at $\theta_\pi = 0^\circ$. The full TR angular distribution, however, has a different shape due to the spin-flip contributions to the cross section. This demonstrates the importance of the second term on the rhs of Eq. (44), which does not vanish but rather reaches its maximum at $\theta_\pi = 0^\circ$. The overall result is quite a flat angular distribution at small pion angles and a falloff at higher angles, which not as steep as the LO component. This behavior of the TR component is very similar to the observed angular distribution in pion photoproduction (γ, π) reactions on the deuteron; see, e.g., Ref. [50].

VI. SUMMARY AND CONCLUSIONS

In summary, we have shown that (p, n) charge-exchange reactions on a deuteron target provide an excellent tool to investigate the ΔN interaction. They probe both the LO and the TR response function in a kinematic region that is inaccessible to real pion or photon reactions. We have presented a coupled-channel approach that allows the theoretical treatment of the interacting ΔN system. By assuming that the Δ resonance is excited dominantly in a direct interaction with the projectile, we modified the coupled equations and showed how to solve for the correlated ΔN wave function in a very efficient way with the Lanczos method. For the ΔN potential, a meson-exchange model was adopted that includes π , ρ , ω , and σ exchange currents.

Results of numerical analysis have been shown for inclusive and exclusive cross sections in the Δ energy region. In the coherent pion production ${}^2\text{H}(p, n \pi^+){}^2\text{H}$, a strong shift of the Δ peak position is observed. We have shown that this lowering in excitation energy is due to the strongly attractive correlations in the LO spin-isospin channel. This attraction emerges mainly from the energy-dependent π -exchange potential. Furthermore, we calculated the angular distribution of the coherent pion component and found it to be strongly forward (in the direction of the momentum transfer) peaked.

The theoretical calculation for the inclusive ${}^2\text{H}(p, n)$ cross section is in fairly good agreement with experimental data. The model describes both the Δ peak and the quasielastic peak very well. In the dip region, theory and measure-

ment agree only in the LO channel, while experimental data are underestimated in the TR channel. The enhancement in the TR channel is most probably due to rescattering effects (i.e., purely mesonic exchange currents). If such effects could explain the shortcomings of the present model, they would also demonstrate the validity limits of the impulse approximation. Therefore, rescattering effects are of special interest and need further investigation. In addition, our model may be improved by including higher nucleon (N^*) resonances in the model space. Both rescattering effects and N^* resonances will be subject of future studies.

ACKNOWLEDGMENTS

We are very grateful to D. L. Prout for making the experimental data available to us. We also thank B. K orfgen for many helpful discussions. This work was supported in part by the Studienstiftung des deutschen Volkes.

APPENDIX A: THE EFFECTIVE PROJECTILE-TARGET-NUCLEON INTERACTION

In Eq. (3) we introduced effective projectile-target-nucleon interactions t_{0j} of which we need explicit representations. The $NN \rightarrow NN$ transition matrix $t_{NN,NN}$ is given in Ref. [51]. Neglecting the small spin-orbit and no-spin transfer components [52,34], we can approximate the spin-isospin part of $t_{NN,NN}$ in the NN c.m. frame by

$$t_{NN,NN}(s,t) = [\alpha(\vec{\sigma}_i \cdot \hat{q})(\vec{\sigma}_j \cdot \hat{q}) + \beta(\vec{\sigma}_i \times \hat{q}) \cdot (\vec{\sigma}_j \times \hat{q})] \vec{\tau}_i \cdot \vec{\tau}_j, \quad (\text{A1})$$

where the unit vector \hat{q} is connected to the initial and final nucleon momenta \vec{k} and \vec{k}' by $\hat{q} = \vec{k} - \vec{k}'$. The coefficients α and β are functions of the Mandelstam variables s and t and describe the strength of LO and TR spin excitations, respectively. They are determined from experimental $pn \rightarrow np$ scattering data [3], which can be fitted with

$$\alpha = c_\alpha \left(\frac{\Lambda_{\alpha 1}^2 + t}{\Lambda_{\alpha 1}^2 - t} \right) \left(\frac{\Lambda_{\alpha 2}^2 - m_\pi^2}{\Lambda_{\alpha 2}^2 - t} \right), \quad (\text{A2})$$

$$\beta = c_\beta \left(\frac{\Lambda_{\beta}^2 - m_\pi^2}{\Lambda_{\beta}^2 - t} \right), \quad (\text{A3})$$

where $c_\alpha = 208 \text{ MeV fm}^3$, $c_\beta = 178 \text{ MeV fm}^3$, $\Lambda_{\alpha 1} = 148 \text{ MeV}$, $\Lambda_{\alpha 2} = 460 \text{ MeV}$, and $\Lambda_\beta = 342 \text{ MeV}$.

The $NN \rightarrow N\Delta$ transition operator $t_{NN,N\Delta}$ consists in principle of 16 linearly independent terms [53,54]. In the present study, however, we assume the simple form

$$t_{NN,N\Delta}(s,t) = [\gamma(\vec{\sigma}_i \cdot \hat{q})(\vec{S}_j^\dagger \cdot \hat{q}) + \gamma'(\vec{\sigma}_i \times \hat{q})(\vec{S}_j^\dagger \times \hat{q})] \vec{\tau}_i \cdot \vec{T}_j^\dagger, \quad (\text{A4})$$

which is completely analogous to Eq. (A1). As before, the coefficients γ and γ' are adjusted to fit experimental data, here of the $pN \rightarrow n\Delta$ reactions [32], yielding

$$\gamma = \gamma' = c_\gamma \left(\frac{\Lambda_\gamma^2 - m_\pi^2}{\Lambda_\gamma^2 - t} \right), \quad (\text{A5})$$

where $c_\gamma = 488 \text{ MeV fm}^3$ and $\Lambda_\gamma = 650 \text{ MeV}$. The fact that data are explained with $\gamma = \gamma'$ means that the ratio LO/TR is 1/2. In spite of their simplicity, the assumed t_{0j} can reproduce not only the cross sections but also the spin observables from the reactions with the proton target. For more details see Ref. [10].

APPENDIX B: EVALUATION OF MATRIX ELEMENTS

All matrix elements that appear in this work are evaluated by using partial-wave expansions and standard tensor operator techniques; see, e.g., Ref. [55]. In this appendix we discuss in some detail the calculation of the radial source function and of the matrix elements for the ΔN interaction. The matrix elements of Sec. IV are not given explicitly but can be calculated rather easily within the presented scheme.

1. Explicit formulas for the source functions

For the ΔN system, the radial source function is obtained from Eq. (24) by inversion

$$\rho_{SLJM_J}(r) = r \langle (SL)JM_J | \rho_\Delta \rangle = r \langle (SL)JM_J | \hat{\rho} | \Psi_d \rangle, \quad (\text{B1})$$

where the deuteron wave function is given as

$$|\Psi_d \rangle = \sum_{l_d=0,2} \frac{1}{r} \phi_{l_d}(r) |(1l_d)1M_d \rangle. \quad (\text{B2})$$

The hadronic transition operator $\hat{\rho}$ was defined in Eq. (8). If we apply the specific form of $t_{NN,N\Delta}$ as given in Eq. (A4) and use the tensor operator notation, $\hat{\rho}$ may be rewritten as

$$\hat{\rho} = \mathcal{I} \sum_{l,m,\nu} \hat{\rho}_{lm\nu}(r) (S_1^\dagger)_\nu^{(1)} Y_{lm}(\hat{r}) + (1 \leftrightarrow 2), \quad (\text{B3})$$

where

$$\hat{\rho}_{lm\nu}(r) = 4\pi \gamma(s,t) (-)^{m_p+1/2} \begin{pmatrix} 1 & \frac{1}{2} & \frac{1}{2} \\ \nu & m_n & m_p \end{pmatrix} \times \langle \frac{1}{2} || \vec{\sigma} || \frac{1}{2} \rangle i^l j_l(\frac{1}{2} qr) Y_{lm}^*(\hat{q}) \quad (\text{B4})$$

and \mathcal{I} denotes the isospin factor

$$\mathcal{I} = \langle \Delta N | \langle n | \vec{\tau}_0 \cdot \vec{T}^\dagger | p \rangle | d \rangle = \delta_{1T} \delta_{1M_T} \frac{2}{\sqrt{3}}. \quad (\text{B5})$$

Insertion of Eqs. (B2) and (B3) into Eq. (B1) yields

$$\rho_{SLJM_J}(r) = \mathcal{I} \sum_{l,m,\nu} \tilde{\rho}_{lm\nu}(r) \sum_{l_d} \phi_{l_d}(r) \times \langle (SL)JM_J | (S_1^\dagger)_\nu^{(1)} Y_{lm}(\hat{r}) | (1l_d)1M_d \rangle + (1 \leftrightarrow 2). \quad (\text{B6})$$

The calculation of the angular momentum matrix element is straightforward, but requires some lengthy spin algebra. The final result is

$$\begin{aligned}
& \langle (SL)JM_J | (S_1^\dagger)_\nu^{(1)} Y_{lm}(\hat{r}) | (1l_d)1M_d \rangle \\
&= \sqrt{\frac{3}{4\pi}} \hat{J} \hat{L} \hat{l}_d (-1)^{L+1} (\delta_{S1} + \sqrt{5} \delta_{S2}) \\
&\times \sum_{J_i, M_i} (-1)^{(M_J - M_i)} (2J_i + 1) \\
&\times \begin{pmatrix} l & 1 & J_i \\ m & M_d & -M_i \end{pmatrix} \begin{pmatrix} J_i & 1 & J \\ M_i & \nu & -M_J \end{pmatrix} \begin{pmatrix} l & l_d & L \\ 0 & 0 & 0 \end{pmatrix} \\
&\times \begin{Bmatrix} L & J_i & 1 \\ 1 & l & l_d \end{Bmatrix} \begin{Bmatrix} S & 1 & 1 \\ J_i & J & L \end{Bmatrix}. \quad (\text{B7})
\end{aligned}$$

For the radial source function of the NN system, an equation analogous to Eq. (B6) holds with \vec{S}^\dagger replaced by $\vec{\sigma}$, an isospin factor $\mathcal{I} = \sqrt{2}$, and transition strengths $\alpha(s,t)$ and $\beta(s,t)$, respectively, instead of $\gamma(s,t)$.

2. Matrix elements of the ΔN potential

In configuration space, the ΔN potentials $V_{\Delta N \rightarrow \Delta N}$ (direct) and $V_{\Delta N \rightarrow N\Delta}$ (exchange) as well as the transition potential $V_{\Delta N \rightarrow NN}$ exhibit the spin-isospin structure

$$\begin{aligned}
V_{ab \rightarrow a'b'}(k_0, \vec{r}) &= \mathcal{F}^N(r) + [\vec{\sigma}_1^{aa'} \cdot \vec{\sigma}_2^{bb'} \mathcal{F}^C(r) \\
&\quad + S_{12}^{aa',bb'}(\hat{r}) \mathcal{F}^T(r)] \vec{\tau}_1^{aa'} \cdot \vec{\tau}_2^{bb'}. \quad (\text{B8})
\end{aligned}$$

Here $\vec{\sigma}^{aa'}$ and $\vec{\tau}^{aa'}$ are the appropriate spin and isospin operators with $a, a' \in \{N, \Delta\}$ and

$$S_{12}^{aa',bb'}(\hat{r}) = 3(\vec{\sigma}_1^{aa'} \cdot \hat{r})(\vec{\sigma}_2^{bb'} \cdot \hat{r}) - \vec{\sigma}_1^{aa'} \cdot \vec{\sigma}_2^{bb'} \quad (\text{B9})$$

is the usual spin tensor operator. In terms of the spin operators used in Sec. III, we have $\vec{\sigma}^{NN} = \vec{\sigma}$, $\vec{\sigma}^{N\Delta} = \vec{S}^\dagger$, and $\vec{\sigma}^{\Delta\Delta} = \vec{\Sigma}$; thus the reduced matrix elements are given by

$$\langle \frac{1}{2} || \vec{\sigma}^{NN} || \frac{1}{2} \rangle = \sqrt{6}, \quad (\text{B10})$$

$$\langle \frac{3}{2} || \vec{\sigma}^{N\Delta} || \frac{1}{2} \rangle = 2, \quad (\text{B11})$$

$$\langle \frac{3}{2} || \vec{\sigma}^{\Delta\Delta} || \frac{3}{2} \rangle = 2\sqrt{15}. \quad (\text{B12})$$

Equivalent equations hold for the isospin operators $\vec{\tau}^{aa'}$.

The functions \mathcal{F} of Eq. (B8) are the Fourier transformations of the nonspin, spin-central, and spin-tensor parts of the interaction, i.e.,

$$\mathcal{F}^N(r) = \frac{1}{2\pi^2} \int dk k^2 j_0(kr) V_{ab,a'b'}^N(k_0, k), \quad (\text{B13a})$$

$$\begin{aligned}
\mathcal{F}^C(r) &= \frac{1}{2\pi^2} \int dk k^2 j_0(kr) [V_{ab,a'b'}^{\text{LO}}(k_0, k) \\
&\quad + 2V_{ab,a'b'}^{\text{TR}}(k_0, k)], \quad (\text{B13b})
\end{aligned}$$

$$\begin{aligned}
\mathcal{F}^T(r) &= \frac{-1}{2\pi^2} \int dk k^2 j_2(kr) [V_{ab,a'b'}^{\text{LO}}(k_0, k) \\
&\quad - V_{ab,a'b'}^{\text{TR}}(k_0, k)]. \quad (\text{B13c})
\end{aligned}$$

For the potentials given in Sec. III, these expressions may easily be found analytically. Furthermore, we need the spin matrix elements that are calculated with standard techniques

$$\begin{aligned}
& \langle [(s_{a'} s_{b'}) S' L'] J M_J | \vec{\sigma}_1^{aa'} \cdot \vec{\sigma}_2^{bb'} | [(s_a s_b) S L] J M_J \rangle \\
&= (-1)^{s_a + s_{b'} + S} \delta_{S S'} \delta_{L L'} \begin{Bmatrix} s_{a'} & s_{b'} & S \\ s_b & s_a & S \end{Bmatrix} \langle s_{a'} || \sigma^{aa'} || s_a \rangle \\
&\quad \times \langle s_{b'} || \sigma^{bb'} || s_b \rangle, \quad (\text{B14})
\end{aligned}$$

$$\begin{aligned}
& \langle [(s_{a'} s_{b'}) S' L'] J M_J | S_{12}^{aa',bb'}(\hat{r}) | [(s_a s_b) S L] J M_J \rangle \\
&= \sqrt{30} (-1)^{(S+J)} \hat{S} \hat{S}' \hat{L} \hat{L}' \begin{pmatrix} L & L' & 2 \\ 0 & 0 & 0 \end{pmatrix} \begin{Bmatrix} S' & S & 2 \\ L & L' & J \end{Bmatrix} \\
&\quad \times \begin{Bmatrix} s_{a'} & s_{b'} & S' \\ s_a & s_b & S \\ 1 & 1 & 2 \end{Bmatrix} \langle s_{a'} || \sigma^{aa'} || s_a \rangle \langle s_{b'} || \sigma^{bb'} || s_b \rangle. \quad (\text{B15})
\end{aligned}$$

From Eqs. (B10)–(B15) one can build up the complete expressions for the matrix elements $V_{nn'}(r)$ as defined in Eq. (26), i.e.,

$$\begin{aligned}
V_{nn'}(r) &= \langle [(s_{a'} s_{b'}) S' L'] J M_J | \langle (\tau_a \tau_b) 11 \\
&\quad \times | V_{ab \rightarrow a'b'}(k_0, \vec{r}) | (\tau_a \tau_b) 11 \rangle | [(s_a s_b) S L] J M_J \rangle. \quad (\text{B16})
\end{aligned}$$

-
- [1] D. Contardo *et al.*, Phys. Lett. **168B**, 331 (1986).
[2] D. A. Lind, Can. J. Phys. **65**, 637 (1987).
[3] C. Gaarde, Annu. Rev. Nucl. Part. Sci. **41**, 187 (1991).
[4] C. Gaarde, Nucl. Phys. **A606**, 227 (1996).
[5] D. L. Prout *et al.*, Phys. Rev. Lett. **76**, 4488 (1996).
[6] E. Oset, H. Toki, and W. Weise, Phys. Rep. **83**, 281 (1982).
[7] T. Udagawa, S. W. Hong, and F. Osterfeld, Phys. Lett. B **245**, 1 (1990).
[8] J. Delorme and P. A. M. Guichon, Phys. Lett. B **263**, 157 (1991).

- [9] F. Osterfeld, Rev. Mod. Phys. **64**, 491 (1992).
[10] T. Udagawa, P. Oltmanns, F. Osterfeld, and S. W. Hong, Phys. Rev. C **49**, 3162 (1994).
[11] J. Chiba *et al.*, Phys. Rev. Lett. **67**, 1982 (1991).
[12] T. Hennino *et al.*, Phys. Lett. B **303**, 236 (1993).
[13] P. Oltmanns, F. Osterfeld, and T. Udagawa, Phys. Lett. B **299**, 194 (1993).
[14] B. Körfgen, F. Osterfeld, and T. Udagawa, Phys. Rev. C **50**, 1637 (1994).

- [15] P. F. de Cordoba, J. Nieves, E. Oset, and M. J. Vicente-Vacas, *Phys. Lett. B* **319**, 416 (1993).
- [16] P. F. de Cordoba, E. Oset, and M. J. Vicente-Vacas, *Nucl. Phys.* **A592**, 472 (1995).
- [17] O. V. Maxwell, W. Weise, and M. Brack, *Nucl. Phys.* **A348**, 388 (1980).
- [18] W. Leidemann and H. Arenhövel, *Nucl. Phys.* **A465**, 573 (1987).
- [19] J. A. Niskanen and P. Wilhelm, *Phys. Lett. B* **359**, 295 (1995).
- [20] P. Wilhelm and H. Arenhövel, *Nucl. Phys.* **A593**, 435 (1995).
- [21] P. Wilhelm and H. Arenhövel, *Nucl. Phys.* **A609**, 469 (1996).
- [22] R. Schmidt, H. Arenhövel, and P. Wilhelm, *Nucl. Phys.* **A355**, 421 (1996).
- [23] S. S. Kamalov, L. Tiator, and C. Bennhold, *Phys. Rev. C* **55**, 88 (1997).
- [24] A. M. Green, in *Mesons in Nuclei*, edited by M. Rho and D. H. Wilkinson (North-Holland, Amsterdam, 1979), Chap. 6, p. 258.
- [25] J. A. Niskanen, *Nucl. Phys.* **A298**, 417 (1978).
- [26] T.-S. H. Lee, *Phys. Rev. C* **29**, 195 (1984).
- [27] T.-S. H. Lee and A. Matsuyama, *Phys. Rev. C* **36**, 1459 (1987).
- [28] H. Pöpping, P. U. Sauer, and X.-C. Zhang, *Nucl. Phys.* **A474**, 557 (1987).
- [29] M. T. Peña, H. Garcilazo, U. Oelfke, and P. U. Sauer, *Phys. Rev. C* **45**, 1487 (1992).
- [30] L. D. Fadeev, *Zh. Eksp. Teor. Fiz.* **12**, 1014 (1961).
- [31] F. Blaazer, B. L. G. Bakker, and H. J. Boersma, *Nucl. Phys.* **A590**, 750 (1995).
- [32] D. L. Prout (private communication).
- [33] D. L. Prout *et al.*, *Nucl. Phys.* **A577**, 233c (1994).
- [34] B. K. Jain and A. B. Santra, *Phys. Rep.* **230**, 1 (1993).
- [35] Y. Jo and C.-Y. Lee, *Phys. Rev. C* **54**, 952 (1996).
- [36] M. Lacombe *et al.*, *Phys. Rev. C* **21**, 861 (1980).
- [37] M. Lacombe, B. Loiseau, R. Vinh Mau, J. Côté, P. Pirés, and R. de Tourreil, *Phys. Lett.* **101B**, 139 (1981).
- [38] R. Machleidt, K. Holinde, and C. Elster, *Phys. Rep.* **149**, 1 (1987).
- [39] G. E. Brown and W. Weise, *Phys. Rep.* **22**, 281 (1975).
- [40] G. F. Chew and F. E. Low, *Phys. Rev.* **101**, 1570 (1956).
- [41] C. A. Mosbacher, Diploma thesis, University of Bonn, 1995 (unpublished).
- [42] X. Y. Chen *et al.*, *Phys. Rev. C* **47**, 2159 (1993).
- [43] H. Esbensen and T.-S. H. Lee, *Phys. Rev. C* **32**, 1966 (1985).
- [44] G. Glass *et al.*, *Phys. Lett.* **129B**, 27 (1983).
- [45] C. Ellegaard *et al.*, *Phys. Lett. B* **231**, 365 (231).
- [46] J. S. O'Connell *et al.*, *Phys. Rev. C* **35**, 1063 (1987).
- [47] S. Boffi, C. Giusti, and F. D. Pacatti, *Phys. Rep.* **226**, 1 (1993).
- [48] J. W. V. Orden and T. W. Donnelly, *Ann. Phys. (N.Y.)* **131**, 451 (1981).
- [49] C.-Y. Lee, *Phys. Rev. C* **55**, 349 (1997).
- [50] T. Ericson and W. Weise, *Pions and Nuclei* (Clarendon, Oxford, 1988).
- [51] A. K. Kerman, H. McManus, and R. M. Thaler, *Ann. Phys. (N.Y.)* **8**, 551 (1959).
- [52] W. G. Love and M. A. Franey, *Phys. Rev. C* **24**, 1073 (1981).
- [53] J. P. Auger, C. Lazard, R. J. Lombard, and R. R. Silbar, *Nucl. Phys.* **A442**, 621 (1985).
- [54] L. Ray, *Phys. Rev. C* **49**, 2109 (1994).
- [55] A. R. Edmonds, *Angular Momentum in Quantum Mechanics* (Princeton University Press, Princeton, 1957).